

Optically Stimulated Luminescence Nanodots experimental determination of bowtie filter shape in computed tomography

A. Khallouqi^{1,2,3*}, W. Allioui¹, A. Halimi¹, O. El rhazouani¹, S. Didi²

¹Hassan First University of Settat,, High Institute of Health Sciences, Laboratory of Health Sciences and Technologies, Settat, Morocco

²Department of radiology public hospital, Mediouna, Morocco

²Department of radiology private clinic Hay Mouhamadi, Casablanca, Morocco

⁴LPMR, Department of Physics, Mohammed Premier University, B.P. 717, Oujda, Morocco

ABSTRACT

► Technical note

*Corresponding author:

Abdellah Khallouqi, Ph.D.,

E-mail: a.khallouqi@uhp.ac.ma

Received: February 2023

Final revised: July 2023

Accepted: August 2023

Int. J. Radiat. Res., January 2024;
22(1): 207-211

DOI: 10.52547/ijrr.21.29

Keywords: Computed tomography (CT) dosimetry, bow-tie filter, OSL dosimeter.

Background: Computed tomography (CT) scans have become an essential diagnostic tool, but they carry significant risks due to the exposure of patients to ionizing radiation. Therefore, healthcare professionals have a responsibility to optimize radiation dose and image quality simultaneously. One factor that significantly affects the quality of images and radiation dose is the bowtie filter used in CT systems, which homogenizes and shapes the X-ray spectrum. However, its characteristic shape, specific to each manufacturer makes it impossible to model it from only the information in the technical note alone. **Materials and Methods:** This study presents a novel methodology using optically stimulated luminescence (OSLD) nanodots to determine the body bowtie filter shape in a Siemens SOMATOM EMOTION 16-slice CT. The accuracy of the body bowtie filter shape generated by OSLD was validated by performing Monte Carlo simulations of CT scans. **Results:** The difference between simulated and measured CTDI_w values for the PET/CT Siemens at 80, 110 and 130 kVp were 4.02%, 7.74%, and 4.81%, respectively. **Conclusion:** In this work, it has been demonstrated that the use of OSLD nanodots allows for the determination of the shape of bowtie filters in CT scans with acceptable accuracy. This work has the potential to address a significant gap in the modeling of bowtie filters, which could significantly improve the optimization of radiation dose and image quality in CT scans.

INTRODUCTION

Computed tomography (CT) is a widely used medical imaging modality that provides valuable diagnostic information ⁽¹⁾. However, CT imaging involves much higher radiation doses than conventional radiography ⁽²⁾. The increasing use of CT scans has raised concerns regarding population exposure to ionizing radiation and long-term health risks such as radiation-induced carcinogenesis ⁽³⁾. To deepen the medical community's comprehension of the potential hazards linked to CT examinations, experts have endeavored to quantify the radiation exposure levels experienced by individual patients. This necessitates the gathering of comprehensive data on the system's energy spectra, which is essential in obtaining precise radiation dose estimations using Monte Carlo simulation (MC) methods ⁽⁴⁾. In turn, comprehending the energy spectra entails a commanding grasp of the deployed filters that uniformly improve the hardness of the X-ray beam. Regrettably, information detailing the design, shape, and composition of these filters is categorically deemed privatized. The bowtie filter is an essential component of CT scanners that helps

reduce patient dose while maintaining image quality ⁽⁵⁾. The use of that filter can reduce radiation dose by up to 65% compared to scans without the filter ⁽⁶⁾.

Despite their effectiveness, there are concerns about potential variations in bowtie filter shapes and materials across scanner models that can impact dose calculations and image quality. Many studies have aimed to determine simplified bowtie filter shapes and profiles for dosimetry purposes. Boone *et al.* proposed a method to evaluate bowtie filter attenuation profiles using real-time dosimeter measurements ⁽⁷⁾. Turner *et al.* generated equivalent energy spectra and filtration descriptions based on half-value layer measurements that account for bowtie filter filtration ⁽⁸⁾. Belinato *et al.* used the AGMS-D sensor to estimate bowtie filter shapes for Siemens Biograph 16 and GE Discovery VCT PET/CT scanners (General Electric Medical Systems), showing ~4% differences between measured and simulated CT dose index values ⁽⁹⁾. The Time-Resolved Integrated Charge method was used to characterize bowtie filters in CT scanners at the Physikalisch-Technische Bundesanstalt ⁽¹⁰⁾. Bruce *et al.* presented a method using radiochromic films to measure bowtie filter profiles with a maximum 25% relative

error⁽¹¹⁾.

In this study, the focus is on developing a new and cost-effective approach to determine the equivalent body bowtie filter in a Siemens SOMATOM EMOTION 16-slice CT scanner using optically stimulated luminescence detectors (OSLD). The accuracy of the resulting bowtie filter thickness is then assessed by comparing the results of the Computed Tomography Dose Index weighted (CTDI_w) received from MC simulations and the one recovered by experimental measurements. A body CTDI phantom was used for the experiment and an MC code has been performed for the simulation of the CT scan. The proposed method offers a solution to the challenge of bowtie filter shaping, which can help reduce radiation exposure and improve patient safety.

METHODS AND MATERIALS

CT scanner model

The present study utilized a Siemens SOMATOM EMOTION 16-slice CT scanner equipped with two bowtie filters positioned between the X-ray tube and collimation system. The scanner operates in both axial and helical modes at tube voltages of 80 kVp, 110 kVp and 130 kVp. The X-ray tube was located at a distance of 535 mm from the isocenter of the gantry, and possessed an anode angle of 7 degrees. Notably, tube current ranged from 10 mAs to 600 mAs.

Bowtie filter calculation

The OSLD nanodot and the associated MicroStar reader have been used in this study (nanodots, Landauer Inc., Glenwood, IL). The sensitive volume of the nanoDot OSLD is a fine pellet of compacted carbon-doped alumina powder (Al₂O₃: C) of 4 mm diameter and 1 mm thickness. Each nanoDot has a specific sensitivity that depends on the manufacturing method of the original batch^(12,13).

In this study, 34 nanoDot dosimeters were utilized - 30 for data acquisition and 4 for calibration purposes. The OSLD chips were positioned in a single 3×60 cm² polymethyl methacrylate (PMMA) slice with a thickness of 3 mm. The device contained 30 square cavities, each 10mm in diameter and 1mm deep, spaced 1 cm apart figure 1. The tolerance for all dimensions in the custom-fabricated device was ± 0.1 mm.

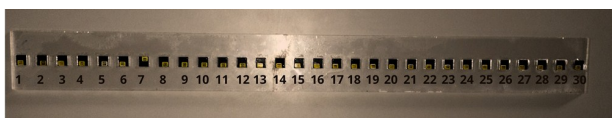


Figure 1. Placement of 30 numbered optically stimulated luminescence dosimeter chips in a PMMA ruler.

The CT gantry was fixed at the 12 o'clock position, with the ruler was placed at a distance of 20 cm from the gantry isocenter. Chip number 15 was centered within the axial field of view (FOV). The OSLD chips

were aligned using the gantry laser, and the CT scanner was set to a routine abdomen protocol to program. The scan parameters were 110 kVp tube voltage, 100 mAs tube current, and 1 s exposure time.

The attenuation by the bowtie filter is taken into account by assigning an air kerma ($K_{meas,E}$) to every photon leaving the x-ray source through the bowtie filter and subsequently reaching the OSLD, given by:

$$K_{Meas,E}(\theta) = K_{(0,E)} * exp^{-\mu_{Al(E)}Y_{n(Al)}} \quad (1)$$

Where $K_{(0,E)}$ is the start air kerma of the photon, $\mu_{Al(E)}$ represents the linear attenuation coefficient of aluminum, and $Y_{n(Al)}$ is the thickness of bowtie filter ($n=1, 2, 3 \dots 31$ OSLD numbers). It's important to note that equation 1 assumed that the bowtie filter consisted of aluminum. For solving equation 1 and finding $Y_{n(Al)}$, $\mu_{Al(E)}$ value was determined by using the following equation 2.

$$\mu_{Al(E)} = 0.693/HVL \quad (2)$$

Half-Value Layer (HVL) refers to the thickness of a material required to reduce radiation intensity by half. The HVL value was determined experimentally using an ionization chamber at 110 kVp.

The absorbed radiation doses ($K_{meas,E}$) measured by each of the 30 optically stimulated luminescent detectors positioned along the path of the X-ray photons have been used to calculate the thickness of the bowtie filter material ($Y(n)$) in the direction of X-ray photon travel. The data obtained are then adjusted leading to a modeling of the bowtie filter by a polynomial function of the second degree⁽¹⁴⁾.

Physical measurement of the CTDI_w phantom

CTDI_w has been measured by using a body PMMA phantom (32 cm diameter, 15 cm of length, a density of $\rho = 1.19$ g/cm³ and five holes located at the center, 3h, 6h, 9h, 12h)⁽¹⁵⁾. A Calibrated pencil ion chamber (model 10×6-3CT RADCAL, USA) connected to an electrometer (RADCAL, USA) have been used; interface software (Accu-Gold+) has been used to show the output of dose, dose rate, time, kVp, Flash HVL, and beam filtration⁽¹⁶⁾.

The body phantom has been aligned with the z-axis of the CT scan. The position of the phantom has been verified with a CT localizer radiograph. The ion pencil chamber has been placed at the center and the other holes of the PMMA phantom figure 2. a. The absorbed dose has been recorded.

$$CTDI_w = \frac{1}{3}CTDI_{100c}^c + \frac{2}{3}CTDI_{100p}^p \quad (3)$$

Where $CTDI_{100}$ represents an integrated measurement of radiation output over a 100 mm dose chamber. $CTDI_{100c}$ denotes the $CTDI_{100}$ value measured at the center of the phantom, whereas $CTDI_{100p}$ represents the mean value of four peripheral $CTDI_{100}$ measurements.

Monte Carlo simulation

The experimental results were compared against simulations performed with the Monte Carlo toolkit GATE version 8.1.0 leveraging GEANT4 version 10.3. The physics processes were modeled using the EMLivermore physics list which is optimized for accurate electron and photon transport at low energies. Absorbed dose was determined through the energy deposited, employing the Dose Actor approach (17).

Monte Carlo calculations were performed to simulate a single gantry rotation with a 10 mm beam collimation along the z-axis. The source-to-isocenter distance was fixed at 535 mm. The source energy spectrum was modeled using a 110 kVp spectrum with a 7° anode angle, which was input into the GATE software using the General Particle Source Module (GPSM). The source was defined as an isotropic point source of γ -particles with an angular distribution of $88.72^\circ \leq \varphi \leq 91.28^\circ$ and $62.1^\circ \leq \theta \leq 117.9^\circ$ in spherical coordinate angles φ and θ figure 2. b.

The energy spectra for all modeled tube voltages were generated using the SRS-78 program. Simulating the 0.5 keV X-ray photon energy increments in GATE was quite time-consuming. However, for increased accuracy at the cost of longer computation time, expanding the kVp range to 5 keV increments is recommended (18,19).

In this study, we utilized a method where 30 OSLD chips were placed in a single slice of PMMA within the FOV. The material attenuation coefficient ($\mu(E)$) was then determined by measuring the HVL value using an ion chamber. Based on the OSLD dosimetry

results, we were able to identify the thickness and shape of the body bowtie filter. We then compared the CTDI_w values obtained from both measuring and simulating with this bowtie filter.

RESULTS

Table 1 presents the radiation dose measured in each OSLD. The thickness Y(n) (n=1, 2, 3 ... 30 OSLD numbers) of the bowtie filter was calculated by using equations 1 and 2 and has been shown in the 3 th row of table 1.

Equation 4 was used to fit the data, describing the shape of the body bowtie filter. Figure 3 illustrates the shape of the bowtie filter where X and Y represent the horizontal distance in cm and the thickness of the bowtie filter in mm of aluminum, respectively.

$$Y = 0.0149X^2 - 0.4627X - 4.4346 \tag{4}$$

Figure 4 presents a normalized attenuation profile of the bowtie filter generated by MC simulation. This profile was compared to the corresponding measured profile obtained at 110 kVp. The results showed a strong correlation between the simulated and measured profiles of air kerma at all measurement points. The Root Mean Square Error (RMSE) was calculated to be 0.955%, indicating good agreement between the simulated and measured profiles.

Table 2 show the results of the simulated and measured CTDI_w values and relative difference in 80, 110 and 130 kVp.

Table 1. Normalized air kerma measured using the OSLD and the calculated thickness of the bowtie filter.

OSLD Numbers	1	2	3	4	5	6	7	8	9	10	11	12	13	14	15
Air KERMA (mGy)	0.254	0.298	0.211	0.332	0.367	0.402	0.497	0.563	0.638	0.704	0.761	0.822	0.894	0.957	1.0008
Y(n)(cm)	3.464	3.116	3.867	2.882	2.664	2.466	2.00	1.733	1.462	1.248	1.078	0.911	0.728	0.580	0.048
OSLD Numbers	16	17	18	19	20	21	22	23	24	25	26	27	28	29	30
Air KERMA (mGy)	1.001	0.989	0.949	0.866	0.748	0.682	0.611	0.539	0.479	0.436	0.398	0.353	0.318	0.272	0.231
Y(n)(cm)	0.483	0.509	0.612	0.797	1.116	1.317	1.556	1.828	2.085	2.289	2.487	2.748	2.975	3.315	3.670

OSLD: optically stimulated luminescence detectors

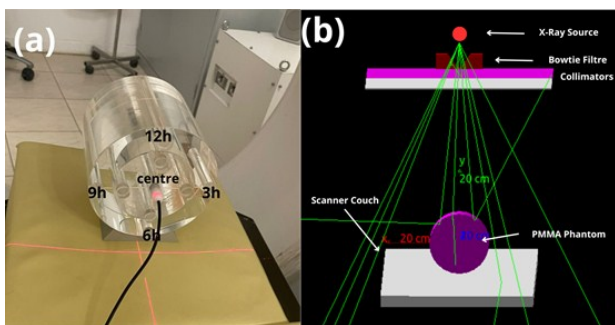


Figure 2. The experimental set-up used to measure CTDI_w using a PMMA phantom (a). Schema of GATE simulation for body phantom (b).

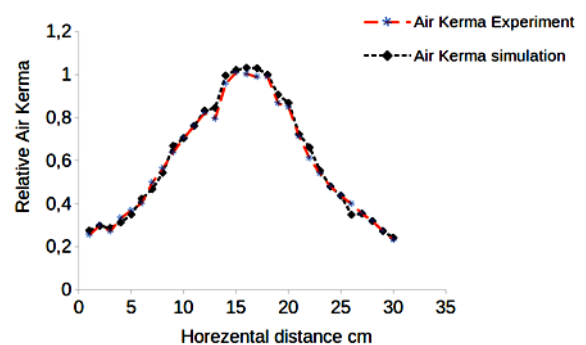


Figure 3. The results of body bowtie filter thicknesses.

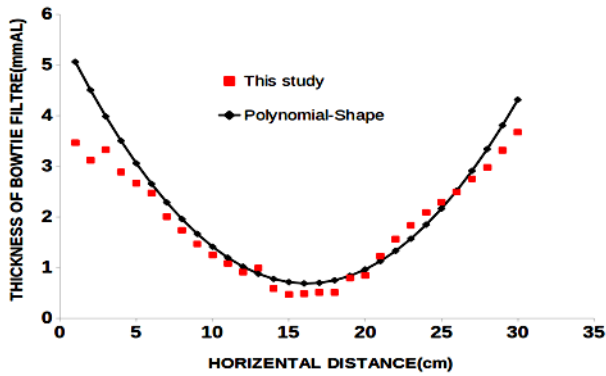


Figure 4. Comparison of normalized profiles between simulated and measured air kerma for 110 kVp.

Table 2. Comparison between simulated and measured CTDI_w for body phantom at 100 mAs for different kVp.

KVp	Measured CTDI _w (mGy)	Simulated CTDI _w (mGy)	% Differences
80	3.23 ± 0.24	3.10 ± 0.023	4.02
110	8.26 ± 0.5	7.62 ± 0.012	7.74
130	11.85 ± 0.72	12.42 ± 0.025	4.81

KVp: kilovolt peak
CTDI_w: Computed Tomography Dose Index weighted

DISCUSSION

The accurate measurement of radiation dose in CT is crucial to ensure patient safety. The current study developed an innovative method to estimate the bowtie filter shape of a CT scanner using OSLD nanodots as dosimeters. The study systematically evaluated the comprehensiveness of this technique by comparing the measured air kerma from a CT localizer radiograph with the simulated air kerma under identical conditions. A comparable level of agreement was noted between the measured and simulated air kerma profiles. The calculated bowtie filter thickness showed remarkable agreement between simulated and measured CTDI_w, with minimal deviations of 4.02%, 7.74%, and 4.81% for tube voltages of 80 kVp, 110 kVp, and 130 kVp, respectively. These variations were primarily attributed to challenges in measurements or errors from external factors such as fluctuations in temperature, pressure or uncertainties in the X-ray spectrum (inherent filtration) used in the simulation.

On the other hand, the shape of the bowtie filters obtained in this study and the study by Hassane *et al.* (20) were systematically compared. Both studies employed physical measurements and calculations to estimate the bowtie filter thickness and compare the measured and simulated air kerma values. However, OSL nanodots were used to estimate the bowtie filter thickness in this study, while an innovative integration method was used in the study by Hassane *et al.* Regarding the results, both studies demonstrated remarkable agreement between the measured and simulated air kerma values, with minimal deviations ranging from 1.4% to 7.74% for

various tube potentials. Nonetheless, the maximum deviations in this study were slightly higher than those in the study by Hassane *et al.* (20)

These results show the high sensitivity, accuracy, and practicality of OSLD for dose measurement. OSLD showed comparable levels of sensitivity to other detectors, while offering key advantages in terms of ease of reuse, accessibility, and cost-effectiveness. The study has also enabled the shape of the bowtie filter for a specific model of PET/CT system to be determined with a high degree of accuracy. This filter shape can be introduced into MC simulations to model the system with minimal error, enabling researchers to accurately determine the true CTDI value through simulations. Given the difficulty of experimental dose measurements for internal organs, the ability to perform accurate MC simulations through the use of this bowtie filter shape will be invaluable for future research in the field of internal organ dosimetry.

ACKNOWLEDGMENTS

The authors would like to thank the Hassan First University for the financial support.

Declarations of interest: The authors confirm they have no conflicts of interest to declare.

Ethical considerations: The study was approved by a number of local institutional ethics committee.

Funding: No financial contribution of any kind has supported this publication

Author contributions: A.K. and W.A. conceived of the presented idea. K.A. conceived and planned the experiments. A.H., S.D. and O.E.R., verified the analytical methods. All authors discussed the results and contributed to the final manuscript.

REFERENCES

1. Samei E and Pelc BJ (2020) Computed tomography. Springer, 2020.
2. Fallah Mohammadi GR, Riyahi Alam N, Geraily G, *et al.* (2016) Thorax organ dose estimation in computed tomography based on patient CT data using Monte Carlo simulation. *Int J Radiat Res*, **14**(4): 313-321.
3. Medicine AA of Pin (2008) The measurement, reporting, and management of radiation dose in CT. AAPM report; 2008.
4. Poirier Y, Kouznetsov A, Koger B, *et al.* (2014) Experimental validation of a kilovoltage X-ray source model for computing imaging dose. *Medical Physics*, **41**(4): 041915.
5. Ahmadi N, Nasrabadi MN, Karimian A, *et al.* (2017) A TLD based method to estimate bowtie filter shape in PET/CT. *Int J Radiat Res*, **15**(4): 383-390.
6. Cao Y, Ma T, de Boer SF, *et al.* (2020) Image artifacts caused by incorrect bowtie filters in cone-beam CT image-guided radiotherapy. *Journal of Applied Clinical Medical Physics*, **21**(7): 153-159.
7. Boone JM (2010) Method for evaluating bow tie filter angle-dependent attenuation in CT: Theory and simulation results. *Medical Physics*, **37**(1): 40-48.
8. Turner AC, Zhang D, Kim HJ, *et al.* (2009) A method to generate equivalent energy spectra and filtration models based on measurement for multidetector CT Monte Carlo dosimetry simulations. *Medical Physics*, **36**(6Part1): 2154-2164.
9. Belinato W, Santos WS, Paschoal CMM, *et al.* (2015) Monte Carlo simulations in multi-detector CT (MDCT) for two PET/CT scanner models using MASH and FASH adult phantoms. *Nuclear Instru-*

- ments and Methods in Physics Research Section A: Accelerators, Spectrometers, Detectors and Associated Equipment. *Elsevier*, **784**: 524-530.
10. Alikhani B and Büermann L (2016) Non-invasive experimental determination of a CT source model. *Physica Medica*, **32**(1): 59-66.
 11. Whiting BR, Evans JD, Dohatcu AC, et al. (2014) Measurement of bow tie profiles in CT scanners using a real-time dosimeter. *Medical Physics*, **41**(10): 101915.
 12. Omar RS, Hashim S, Bradley DA, et al. (2022) Anthropomorphic phantom organ dose assessment using optically stimulated luminescence dosimeters unified in multi-detector computed tomography. *Radiation Physics and Chemistry*, **200**: 110383.
 13. Granville DA, Sahoo N, Sawakuchi GO (2014) Calibration of the Al₂O₃: C optically stimulated luminescence (OSL) signal for linear energy transfer (LET) measurements in therapeutic proton beams. *Physics in Medicine & Biology*, **59**(15): 4295.
 14. Minami K, Matsubara K, Hayashi Y, et al. (2019) Influence of bowtie filter and patient positioning on in-plane dose distribution and image quality in ECG-gated CT. *Nihon Hoshasen Gijutsu Gakkai Zasshi*, **75**(6): 536-545.
 15. Kadavigere R and Sukumar S (2022) Radiation dose optimization for computed tomography of the head in pediatric population—An experimental phantom study. *Int J Radiat Res*, **20**(4):747-751.
 16. Nakamura T, Suzuki S, Takei Y, et al. (2019) Simultaneous measurement of patient dose and distribution of indoor scattered radiation during digital breast tomosynthesis. *Radiography*, **25**(1): 72-76.
 17. Jan S, Benoit D, Becheva E, et al. (2011) GATE V6: a major enhancement of the GATE simulation platform enabling modelling of CT and radiotherapy. *Physics in Medicine & Biology*, **56**(4): 881.
 18. DeMarco JJ, Cagnon CH, Cody DD, et al. (2005) A Monte Carlo based method to estimate radiation dose from multidetector CT (MDCT): cylindrical and anthropomorphic phantoms. *Physics in Medicine & Biology*, **50**(17): 3989.
 19. Zhang H, Kong V, Huang K, et al. (2017) Correction of bowtie-filter normalization and crescent artifacts for a clinical CBCT system. *Technology in Cancer Research & treatment*, **16**(1): 81-91.
 20. Hassan AI, Skalej M, Schlattl H, et al. (2018) Determination and verification of the X-ray spectrum of a CT scanner. *J Med Imag*, **5** (01): 1.

